

The role of weak hydrogen and halogen bonding interactions in the assembly of a series of Hg(II) coordination polymers

Alireza Azhdari Tehrani[†], Ali Morsali^{†*} and Maciej Kubicki[‡]

Supporting Information

Experimental Section.....	Page 2
ORTEP diagrams	Page 5
Similarity relationship between complexes 1-8.....	Page 8
Selected fragments for halogen bonding interaction energy analysis.....	Page 8
Calculated Hirshfeld surface for a fragment of 4 and 8	Page 11
FE-SEM images of complexes 1-8.....	Page 12
Predicted crystal morphologies of complexes 1-8 and their packing.....	page 14
Comparsion between simulated and experimental PXRD.....	page 22
Table S1. Hydrogen bond geometries for complexes 1-8.....	page 25
Table S2. Relative contributions to the Hirshfeld surface area in 1-8.....	Page 26
Table S3. Face lists generated according to the BFDH law.....	page 27

Experimental Section

Syntheses of complexes

The ligands, (*E*)-4-halo-*N*-(pyridin-4-ylmethylene)aniline ligands, L^{4-F}, L^{4-Cl}, L^{4-Br} and L^{4-I}, were prepared using the previously reported method.¹ It should be noted that the analogous HgCl₂ complexes with L^{4-X} ligands would have been of interest here, but could not be studied because no suitable crystals were obtained.

[HgBr₂(L^{4-F})] (**1**)

To a solution of HgBr₂ (0.037 g, 0.1 mmol) in 5 mL methanol, a solution of L^{4-F} (0.020 g, 0.1 mmol) in 5 mL of methanol was added with stirring. The mixture was heated at 40 °C for about 30 minute. Reduction of the solvent volume resulted in the formation of a yellow precipitate. The precipitate was filtered and washed with methanol (3 × 2 mL), and dried in *vacuo*. The solid was then dissolved by boiling in acetonitrile (10 mL) and filtered. Upon slow evaporation of the filtrate at room temperature, crystals of complex **1** for X-ray analysis were obtained after 6 days. In spite of our efforts, no better crystals were obtained in any solvent. (yield 71%). (m.p. = 195-197°C). Anal. calcd for C₁₂H₉Br₂FHgN₂: C, 25.71; H, 1.62; N, 5.00. Found: C, 25.58; H, 1.73; N, 4.88. IR (KBr pellet, cm⁻¹): 1608 ν(C=N); 1478, 1417 ν(C=N)py.

[HgBr₂(L^{4-Cl})] (**2**)

The procedure was similar to the synthesis of **1** except that L^{4-Cl} (0.022 g, 0.1 mmol) was used instead of L^{4-F}. Prism colorless crystals of **2** were formed after 5 days (yield 85%).(m.p. = 188-190°C). Anal. calcd for C₁₂H₉Br₂ClHgN₂: C, 24.98; H, 1.57; N, 4.85. Found: C, 24.85 H, 1.44; N, 4.79. IR (KBr pellet, cm⁻¹): 1616 ν(C=N); 1479, 1417 ν(C=N)py.

[HgBr₂(L^{4-Br})₂] (**3**)

The procedure was similar to the synthesis of **1** except that L^{4-Br} (0.026 g, 0.1 mmol) was used instead of L^{4-F}. Needle colorless crystals of **3** were formed after 3 days (yield 90%).(m.p. = 198-200°C). Anal. calcd for C₂₄H₁₈Br₄HgN₄: C, 32.66; H, 2.06; N, 6.35. Found: C, 32.64 H, 2.01; N, 6.24. IR (KBr pellet, cm⁻¹): 1609 ν(C=N); 1478, 1414 ν(C=N)py.

[HgBr₂(L^{4-I})] (**4**)

The procedure was similar to the synthesis of **1** except that L^{4-I} (0.031 g, 0.1 mmol) was used instead of L^{4-F}. Prism colorless crystals of **4** were formed after 8 days (yield 95%).(m.p. = 183-185 °C). Anal. calcd for C₁₂H₉Br₂HgIN₂: C, 21.56; H, 1.36; N, 4.19. Found: C, 21.5 H, 1.31; N, 4.16. IR (KBr pellet, cm⁻¹): 1615 ν(C=N); 1477, 1411 ν(C=N)py.

[HgI₂(L^{4-F})] (**5**)

The procedure was similar to the synthesis of **1** except that HgI₂ (0.045 g, 0.1 mmol) was used instead of HgBr₂. Prism colorless crystals of **5** were formed after 5 days (yield 90%).(m.p. = 180-182°C). Anal. calcd for C₁₂H₉FHgI₂N₂: C, 22.02; H, 1.39; N, 4.28. Found: C, 22.03 H, 1.38; N, 4.28. IR (KBr pellet, cm⁻¹): 1611 ν(C=N); 1472, 1414 ν(C=N)py.

[HgI₂(L^{4-Cl})] (**6**)

The procedure was similar to the synthesis of **5** except that L^{4-Cl} (0.022 g, 0.1 mmol) was used instead of L^{4-F}. Prism colorless crystals of **6** were formed after 5 days (yield 78%).(m.p. = 179-181°C). Anal. calcd for C₁₂H₉ClHgI₂N₂: C, 21.48; H, 1.35; N, 4.17. Found: C, 21.46 H, 1.34; N, 4.14. IR (KBr pellet, cm⁻¹): 1610 ν(C=N); 1477, 1413 ν(C=N)py.

[HgI₂(L^{4-Br})] (**7**)

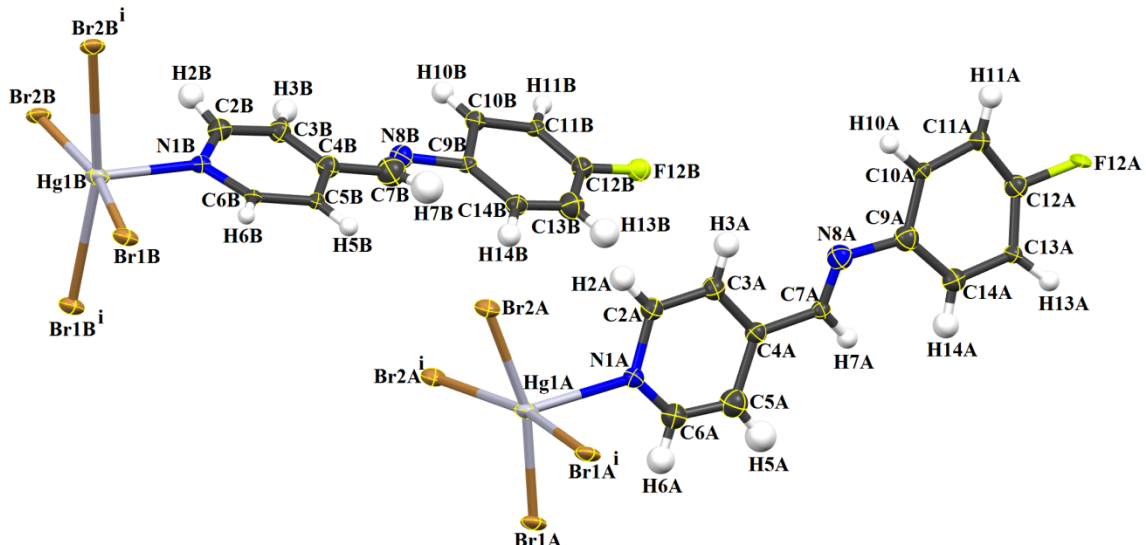
The procedure was similar to the synthesis of **5** except that L^{4-Br} (0.026 g, 0.1 mmol) was used instead of L^{4-F}. Prism colorless crystals of **7** were formed after 5 days (yield 68%).(m.p. = 175-177°C). Anal. calcd for C₁₂H₉BrHgI₂N₂: C, 20.14; H, 1.27; N, 3.92. Found: C, 20.02 H, 1.23; N, 3.85. IR (KBr pellet, cm⁻¹): 1609 ν(C=N); 1470, 1410 ν(C=N)py.

[HgI₂(L^{4-I})] (**8**)

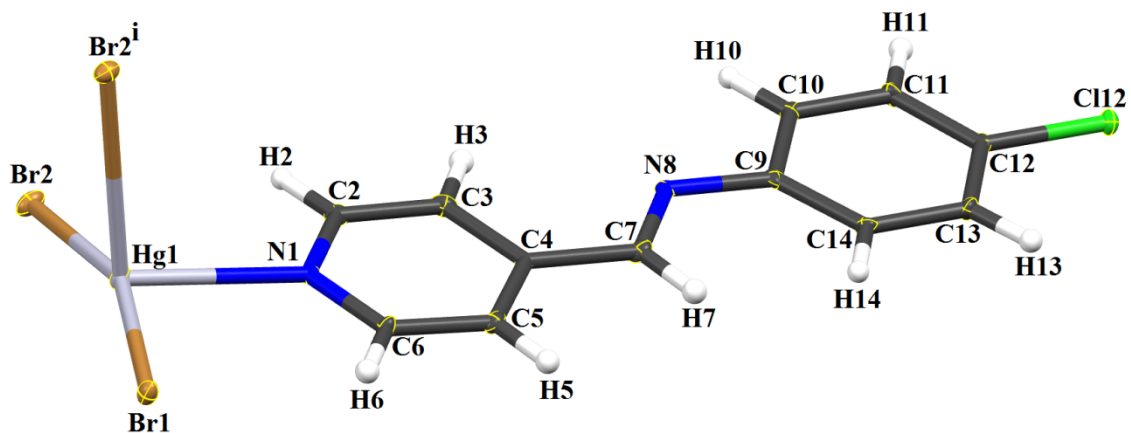
The procedure was similar to the synthesis of **5** except that L^{4-I} (0.031 g, 0.1 mmol) was used instead of L^{4-F}. Prism colorless crystals of **8** were formed after 10 days (yield 82%).(m.p. = 186-188°C). Anal. calcd for C₁₂H₉HgI₃N₂: C, 18.90; H, 1.19; N, 3.67. Found: C, 18.86 H, 1.15; N, 3.64. IR (KBr pellet, cm⁻¹): 1612 ν(C=N); 1470, 1412 ν(C=N)py.

Sonochemical Synthesis of Complexes **1-8.** complexes **1-8**, were readily synthesized by sonochemical method according to the following procedure. 5 ml solution of HgX₂ (X=Br and I) (0.1 mmol) in methanol was positioned in a round bottom flask (50 mL), and then the round bottom flask was fixed in the bath of the ultrasonic generator operating at 40 kHz with a maximum power output of 305W. Into this solution a 5 ml solution of the L^{4-X} (X=F, Cl, Br and I) ligand (0.1 mmol) in methanol was added dropwise. After the ultrasonic irradiation for 15 minutes, the obtained precipitates were filtered off, washed with small amount of methanol, and dried in air. The products were characterized by different techniques such as powder X-ray diffraction (PXRD), IR spectroscopy and elemental analysis. The elemental analysis and FT-IR spectra of the prepared complexes by the sonochemical method and of the conventional method are

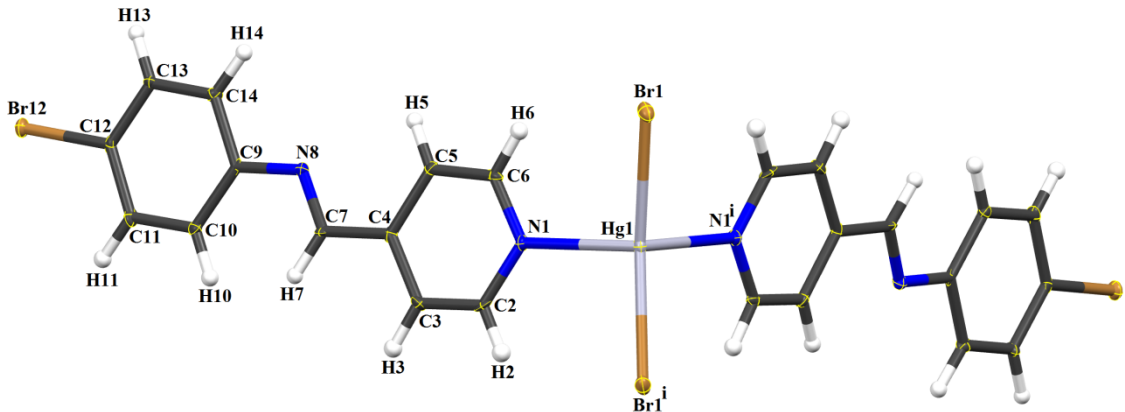
indistinguishable. The morphology and size of prepared products by the sonochemical method were examined by Field-Emission Scanning electron microscopy (FE-SEM).



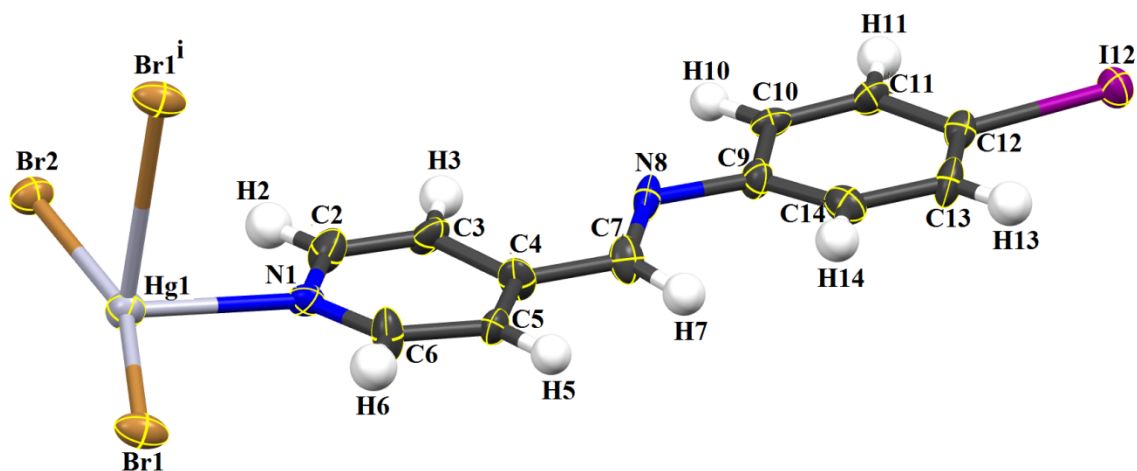
(a)



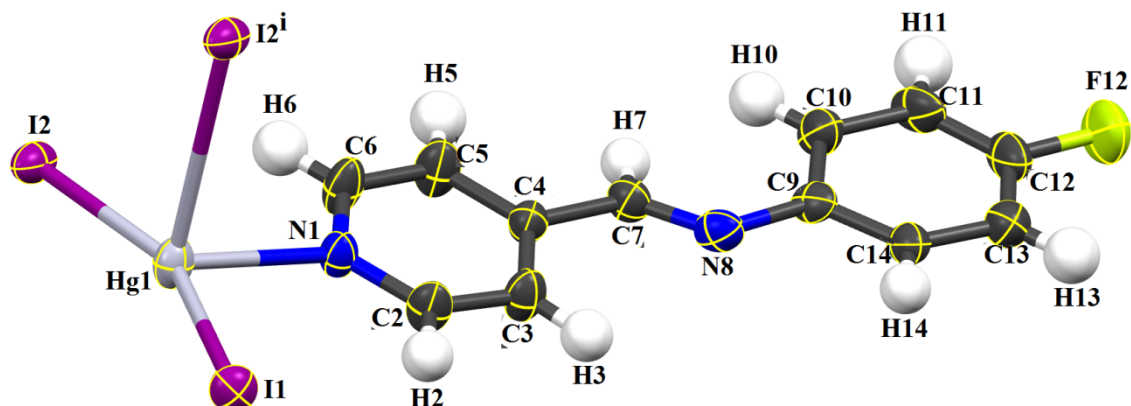
(b)



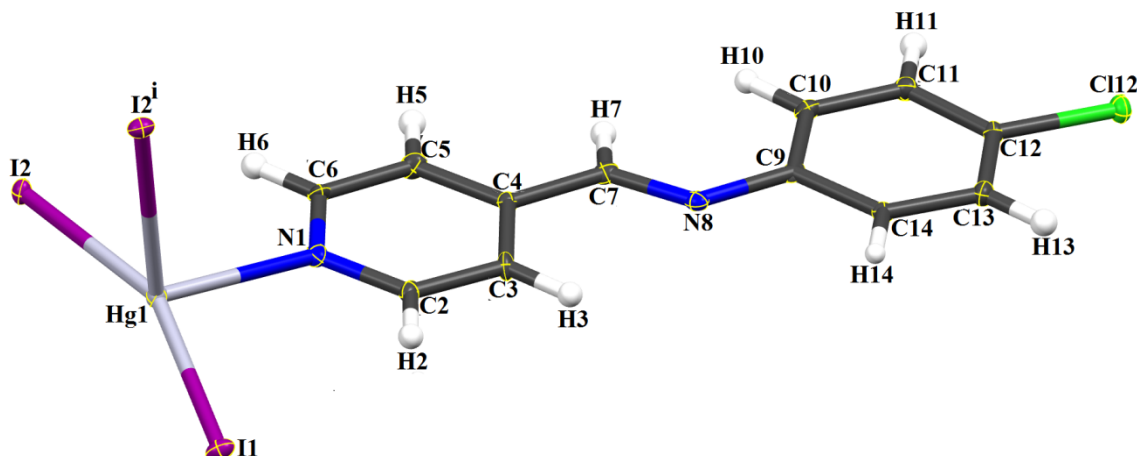
(c)



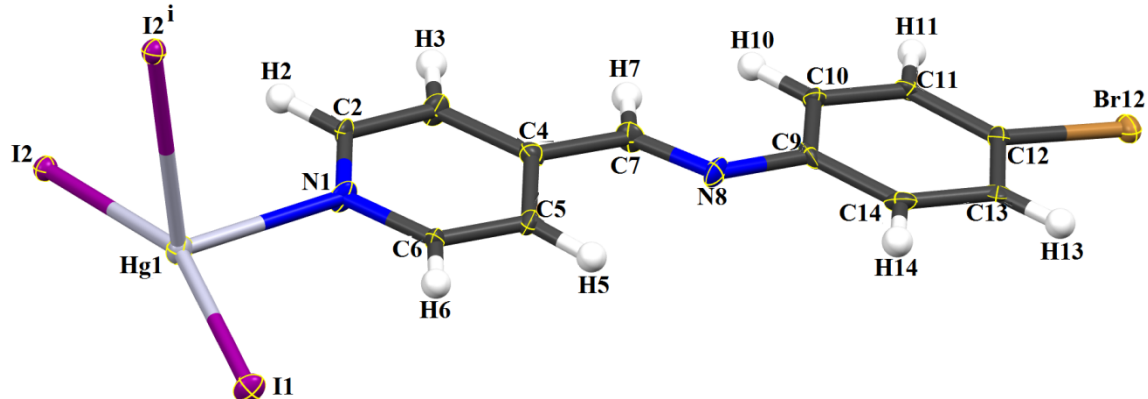
(d)



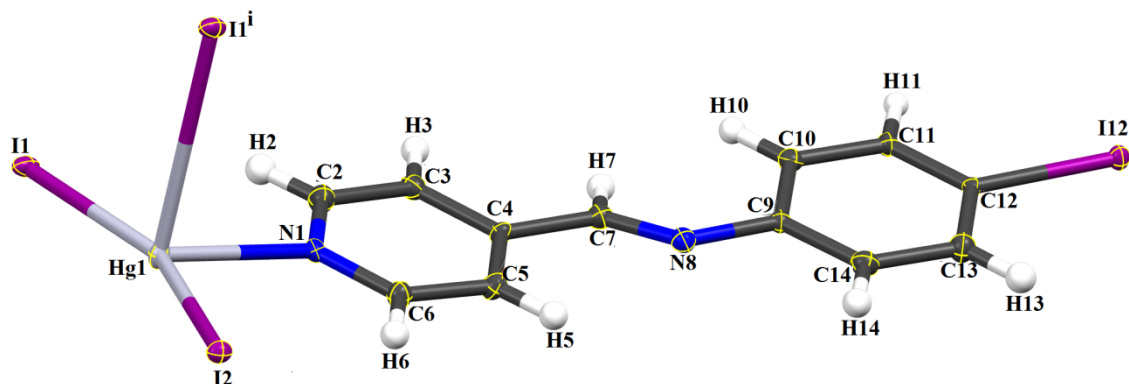
(e)



(f)



(g)



(h)

Figure S1. Portion of the structure of the coordination compounds formed between HgBr_2 and $\text{L}^{4-\text{F}}$, **1**, (a), $\text{L}^{4-\text{Cl}}$, **2**, (b), $\text{L}^{4-\text{Br}}$, **3**, (c), $\text{L}^{4-\text{I}}$, **4**, (d) and between HgI_2 and $\text{L}^{4-\text{F}}$, **5**, (e) $\text{L}^{4-\text{Cl}}$, **6**, (f), $\text{L}^{4-\text{Br}}$, **7**, (g), $\text{L}^{4-\text{I}}$, **8**, (h) showing the coordination geometry around the $\text{Hg}(\text{II})$. Symmetry codes: (a) $\text{Br1B}^i = 1+x, y, z$, $\text{Br2B}^i = -1+x, y, z$, $\text{Br1A}^i = -1+x, y, z$, $\text{Br2A}^i = 1+x, y, z$ (b) $\text{Br2}^i = 1/2+x, 2.5-y, 1-z$ (c) $\text{Br1}^i = -x, 2-y, z$, $\text{N1}^i = -x, 2-y, z$ (d) $\text{Br1}^i = -1+x, y, z$ (e) $\text{I2}^i = x, y, -1+z$ (f) $\text{I2}^i = -1/2+x, 1.5-y, 1-z$ (g) $\text{I2}^i = x, y, 1+z$ (h) $\text{I1}^i = 1+x, y, z$. ORTEP diagrams were drawn by 30% probability.

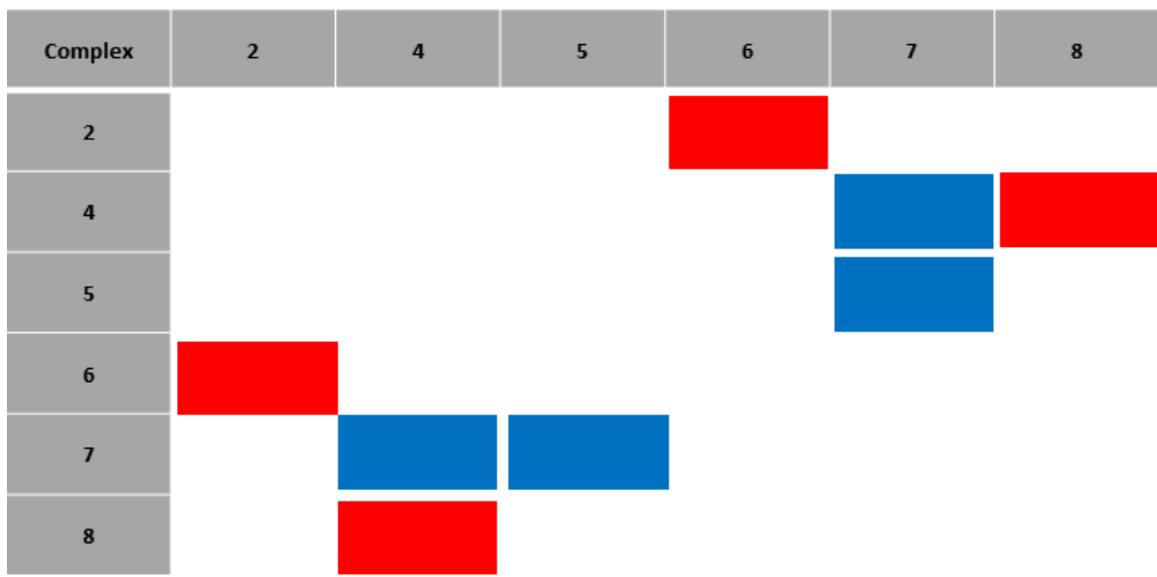
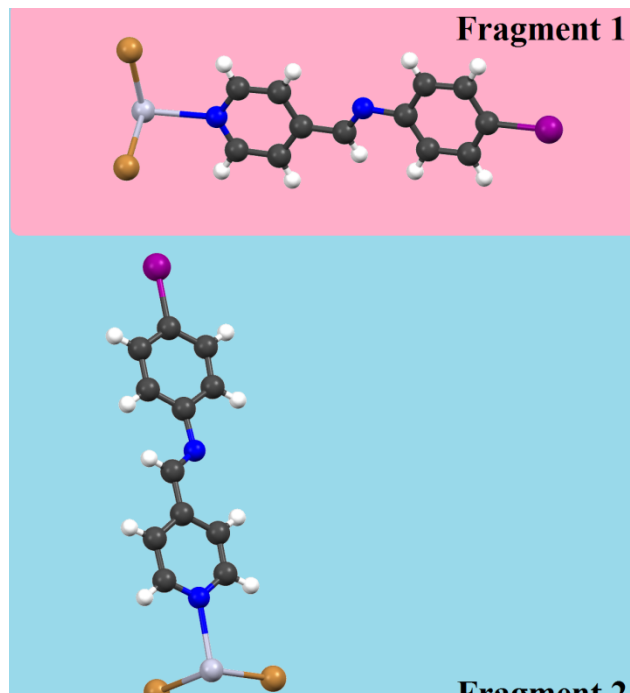
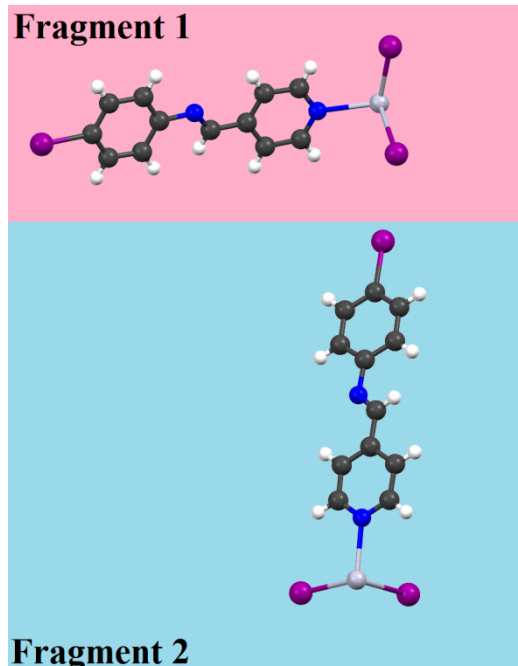


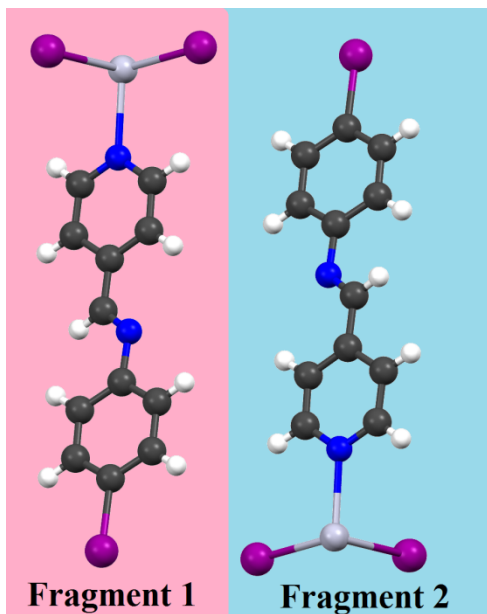
Figure S2. Similarity relationship between complexes **1-8** using XPac analysis. The colour codes are: red = 3D and dark blue = 1D isostructuralty.



(a)



(b)



(c)

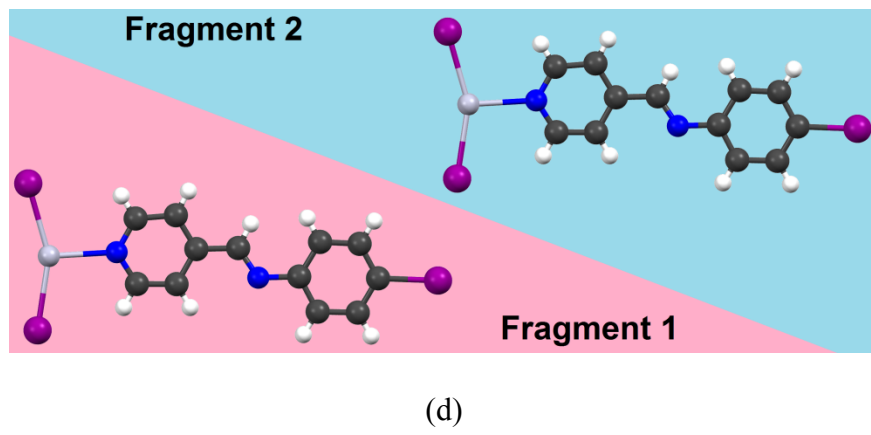


Figure S3. Fragments selected for halogen bonding interaction energy analysis in complexes **4** (a), **8** (b), (c) and (d). Calculations were performed with the experimental structures as the starting point, at the BLYP-D3/TZ2P-ZORA level.

Halogen Bonding geometries and calculated XB binding energies for Compounds **4** (a) and **8** (b-d)

Complex	Interaction	C-I \cdots X-Hg distance	C-I \cdots X angle	Hg-X \cdots I angle	Reduction of the sum of the VDW radii (%)	Symmetry code	Calculated interaction energy	Energy decomposition Analysis
[HgBr ₂ (L ^{4-I})] (a)	C ₁₂ -I ₁₂ ...Br ₁ -Hg ₁	3.580(3)	173.0(7)	110.89(4)	3.25	1-x,1/2+y,2.5-z	-11.61	$\Delta E_{\text{Pauli}} = 31.36$ $\Delta E_{\text{elstat}} = -19.09$ $\Delta E_{\text{orb}} = -11.77$ $\Delta E_{\text{disp}} = -12.11$
[HgI ₂ (L ^{4-I})] (b)	C ₁₂ -I ₁₂ ...I ₁ -Hg ₁	3.697(1)	176.2(5)	112.91(4)	6.65	2-x,-1/2+y,1.5-z	-7.17	$\Delta E_{\text{Pauli}} = 37.18$ $\Delta E_{\text{elstat}} = -21.30$ $\Delta E_{\text{orb}} = -13.89$ $\Delta E_{\text{disp}} = -9.16$
[HgI ₂ (L ^{4-I})] (d)	C ₁₂ -I ₁₂ ...I ₂ -Hg ₁	3.945(2)	96.8(5)	162.95(5)	0.38	3-x,-y,2-z	-21.16	$\Delta E_{\text{Pauli}} = 60.22$ $\Delta E_{\text{elstat}} = -24.12$ $\Delta E_{\text{orb}} = -19.46$ $\Delta E_{\text{disp}} = -37.80$
[HgI ₂ (L ^{4-I})] (d)	C ₁₂ -I ₁₂ ...I ₂ -Hg ₁	3.945(2)	96.8(5)	162.95(5)	0.38	3-x,-y,2-z	-2.44	$\Delta E_{\text{Pauli}} = 23.25$ $\Delta E_{\text{elstat}} = -9.34$ $\Delta E_{\text{orb}} = -6.66$ $\Delta E_{\text{disp}} = -9.68$

It should be noted that the value of the other halogen bonding energy in **8** (selected fragments model (c)) (-21.16 kJ/mol, symm. code: 3-x,-y,2-z) is related to a combination of two C-I \cdots I-Hg and several H \cdots H interactions. Also, the binding energy in **8** (selected fragments model (d)) (-2.44 kJ/mol, symm. code: 3-x,-y,2-z) is obtained when one of the monomers was rotated 180° relative to the other by 180° while keeping the same I \cdots I distance and C-I \cdots I angle. Noteworthy, this interaction is less attractive since the angle requirement is not met and the C-I₁₂ \cdots I₂ distance is close to or slightly below the sum of the van der Waals radii.

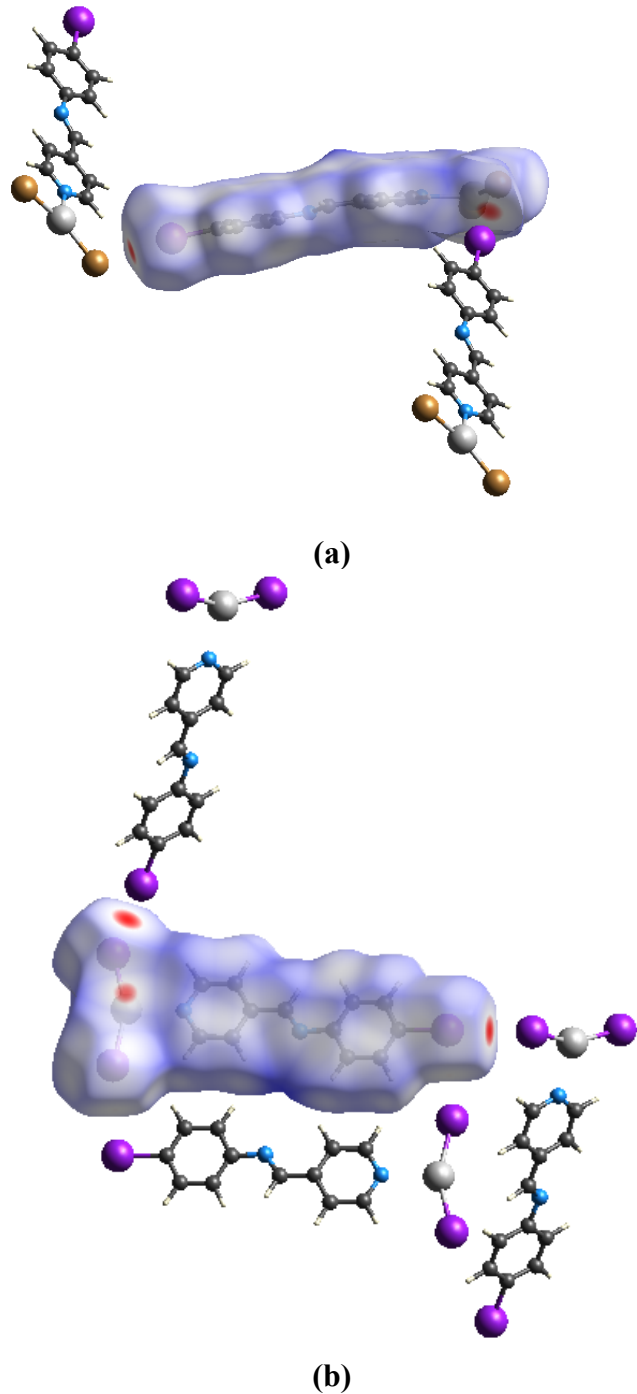
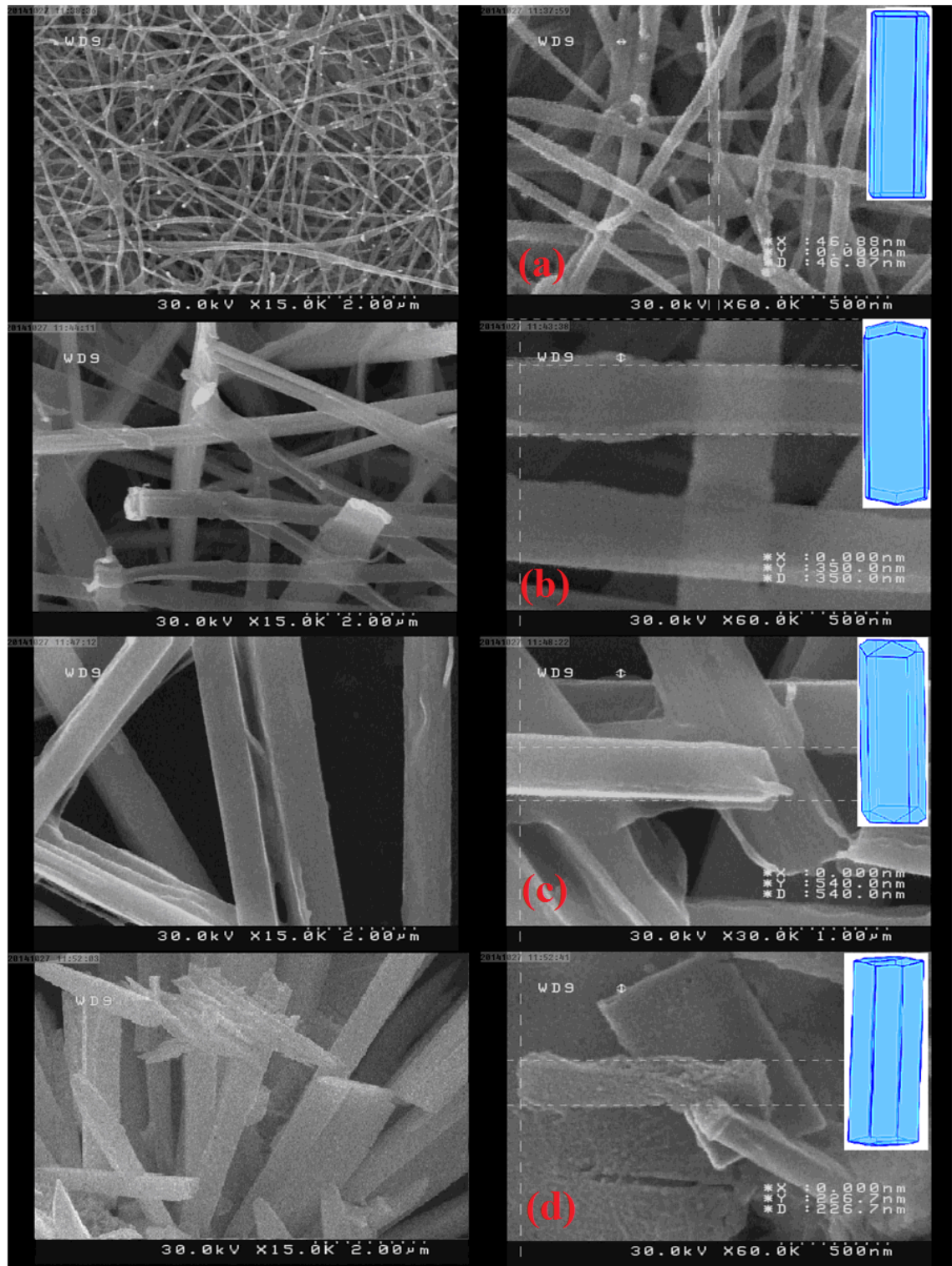


Figure S4. Calculated Hirshfeld surface for a fragment of **4** (a) and **8** (b). The halogen-bonding sites (tips of the C–I) can be seen as large red spots.



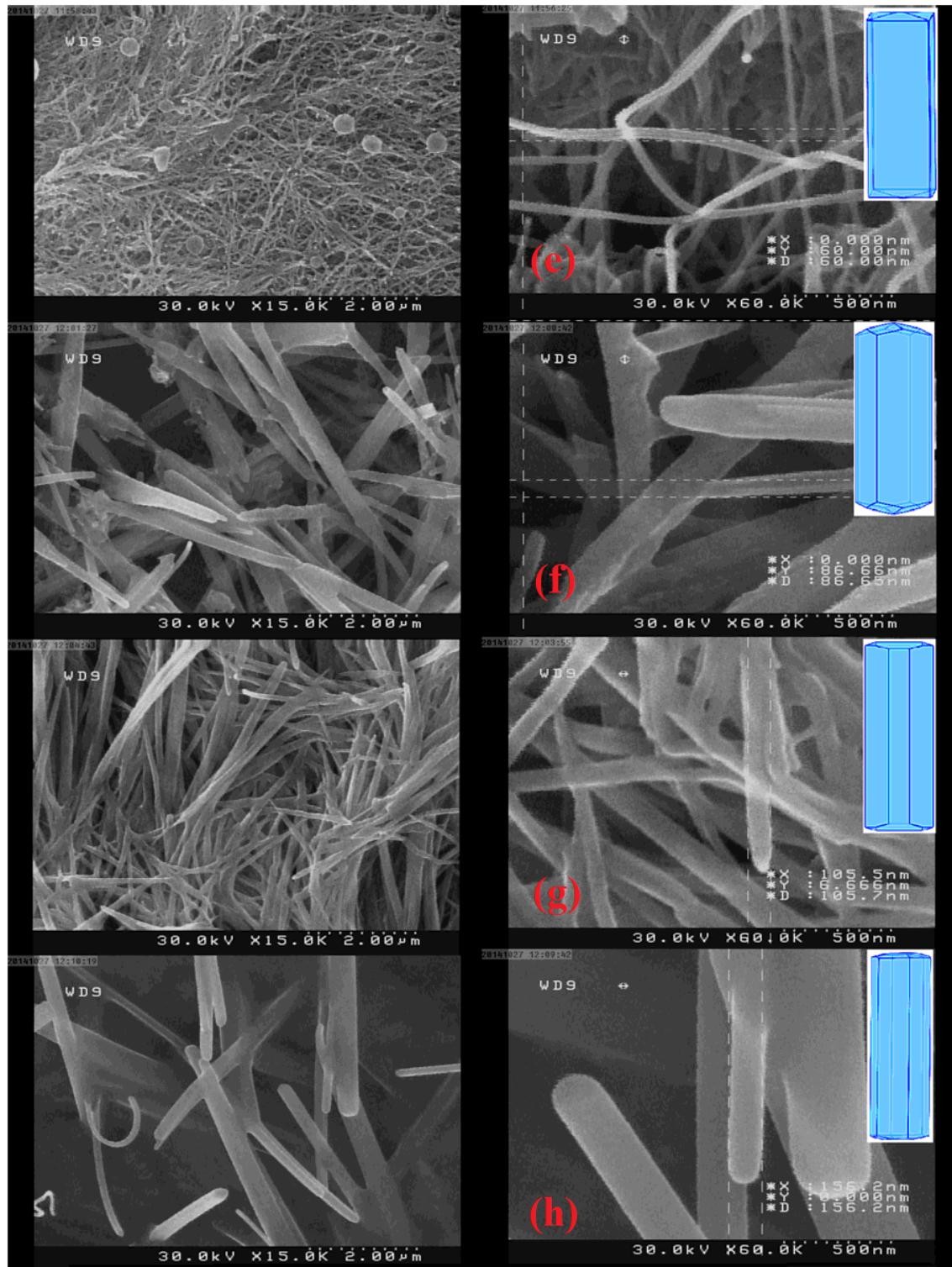
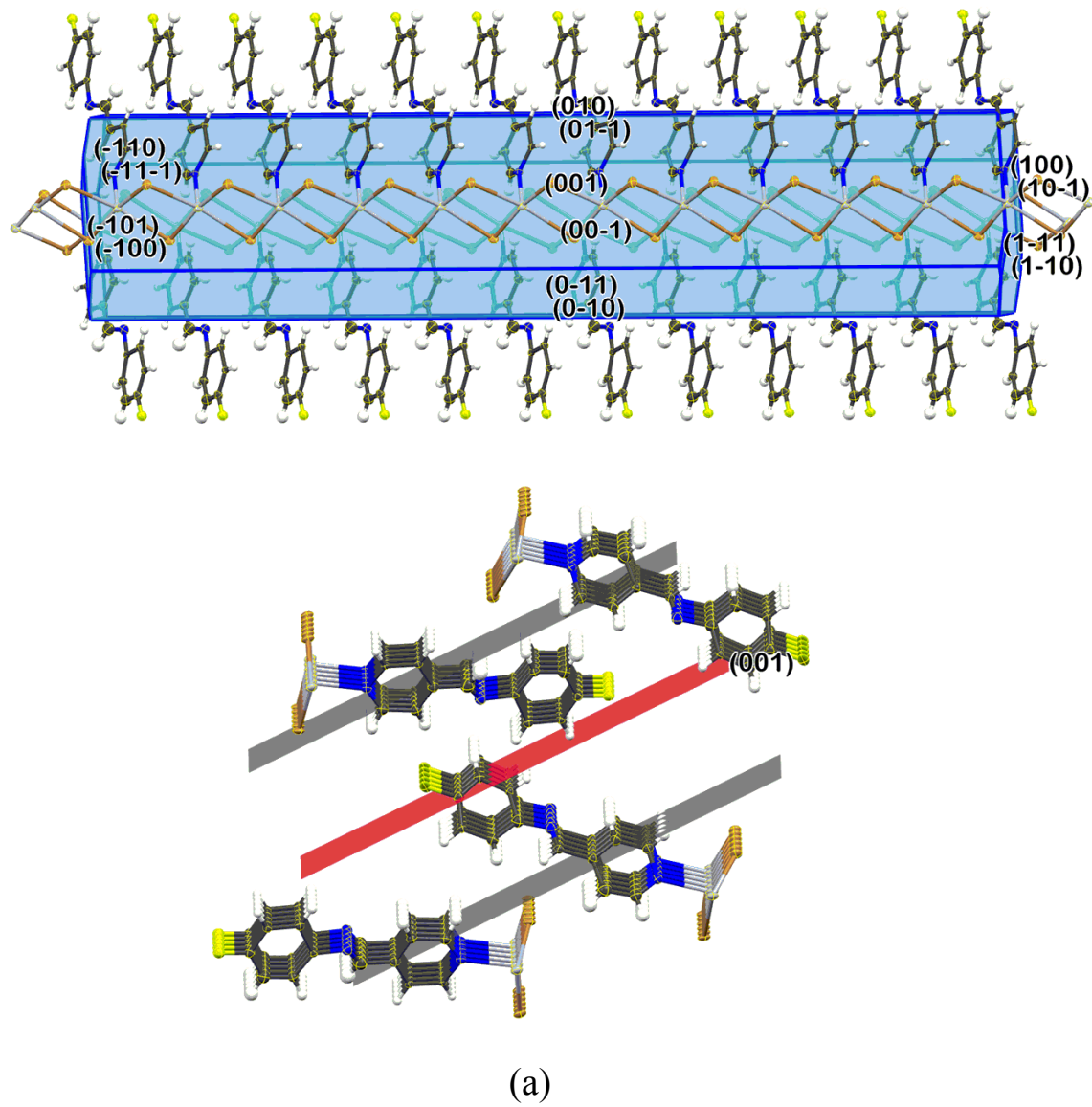
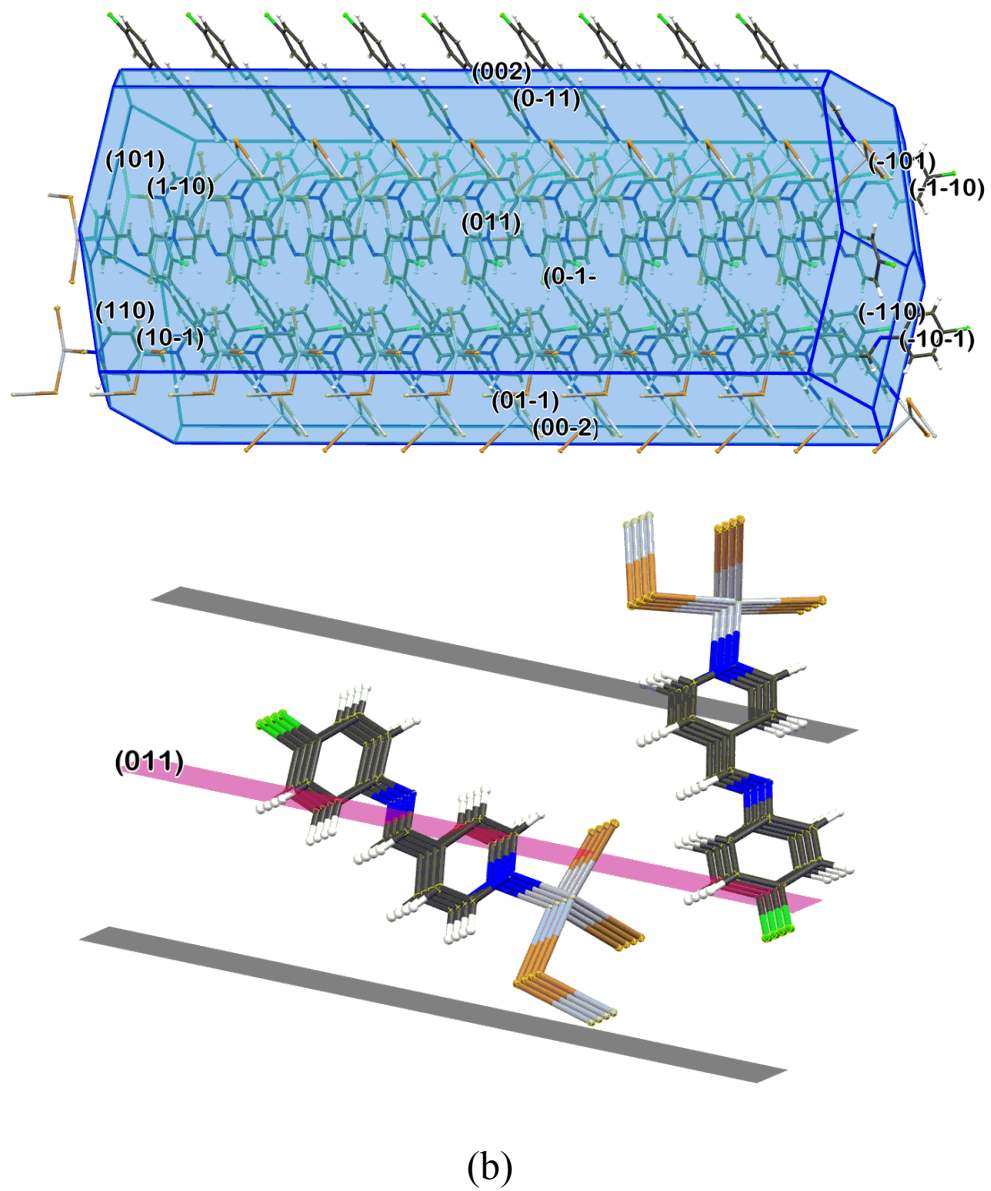
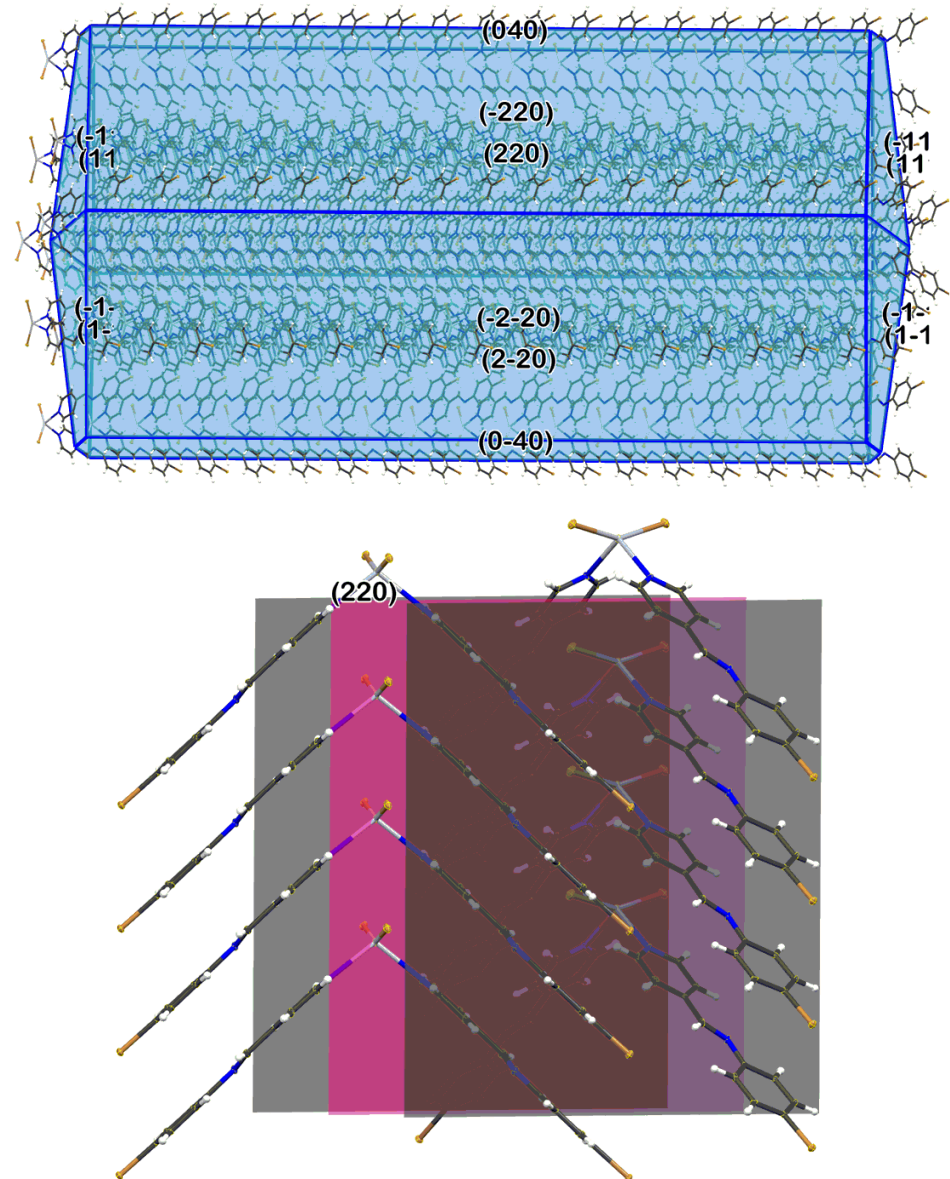


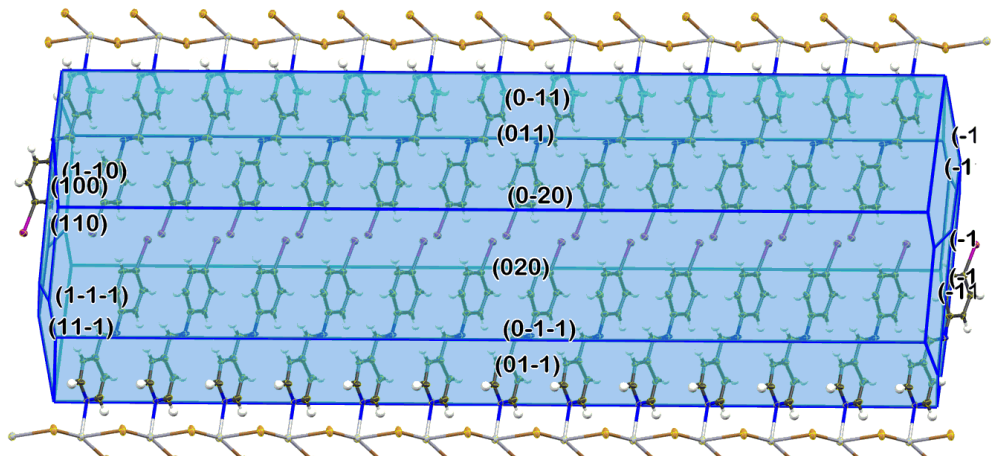
Figure S5. FE-SEM images of complexes **1-8** prepared by ultrasonic generator 305 Win. The right top inserts illustrate the predicted morphology of corresponding complexes **1-8**.
1 (a), **2** (b), **3** (c), **4** (d), **5** (e), **6** (f), **7** (g), **8** (h)



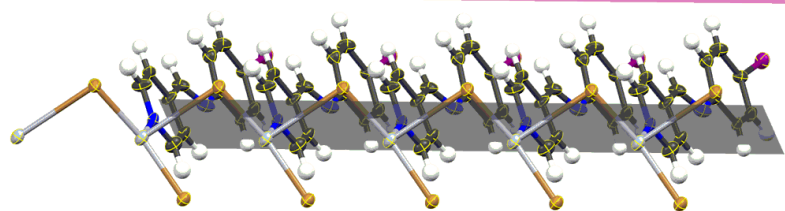




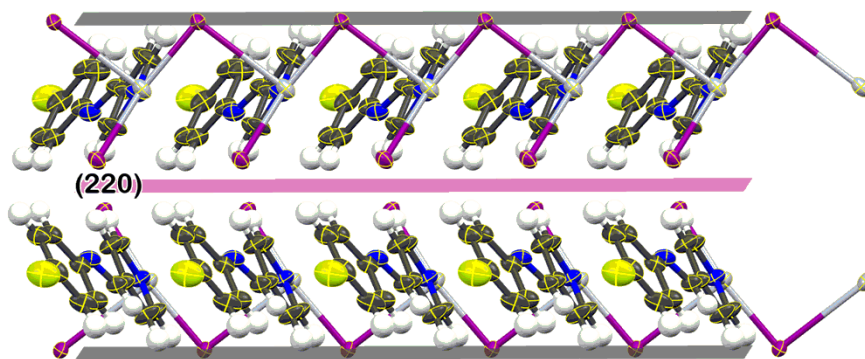
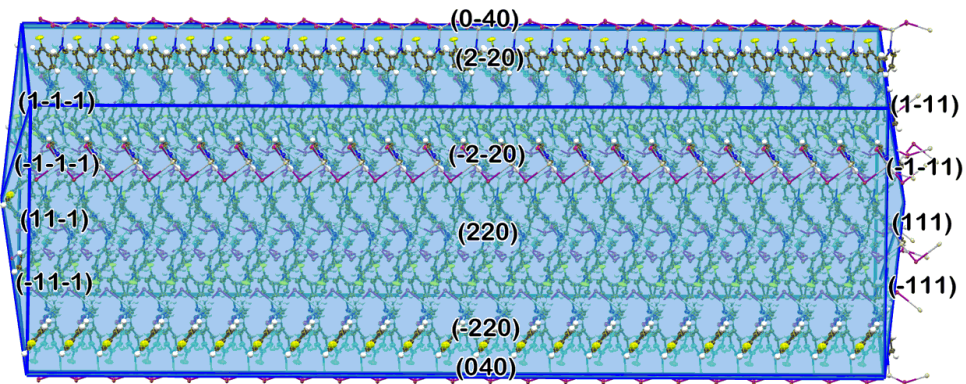
(c)



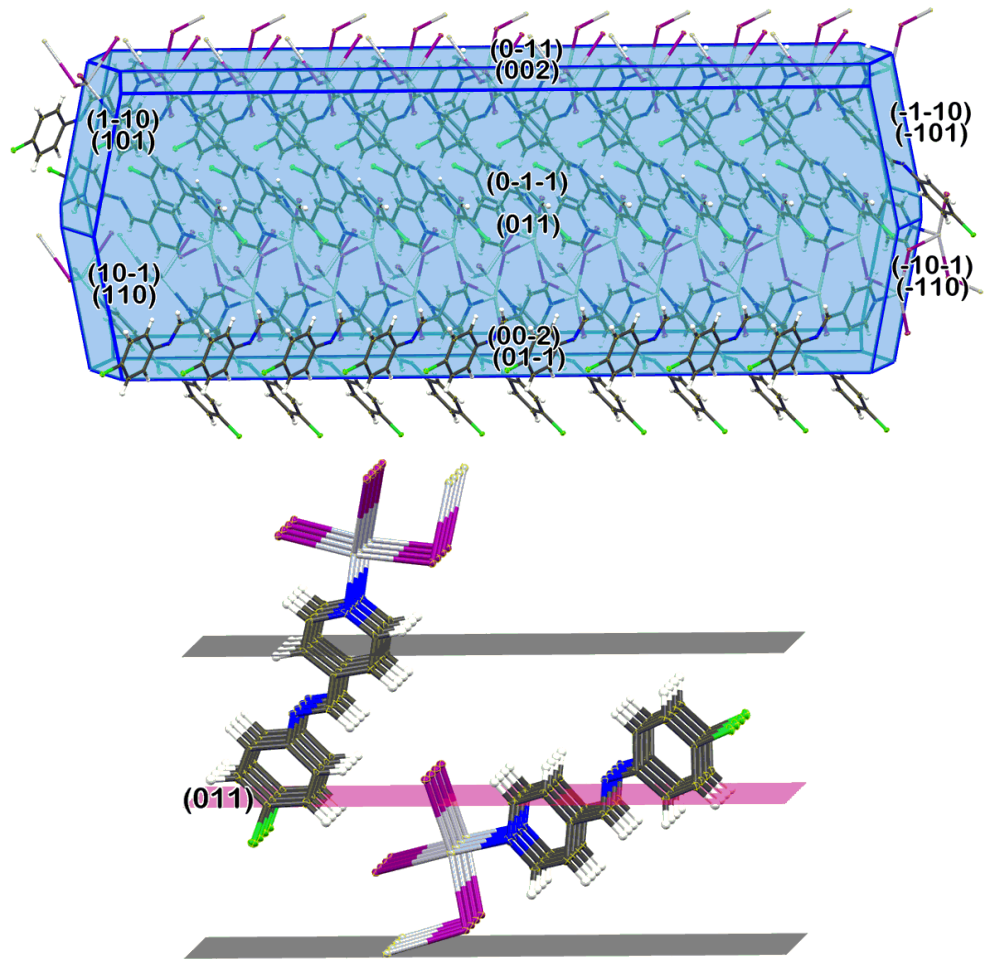
(011)



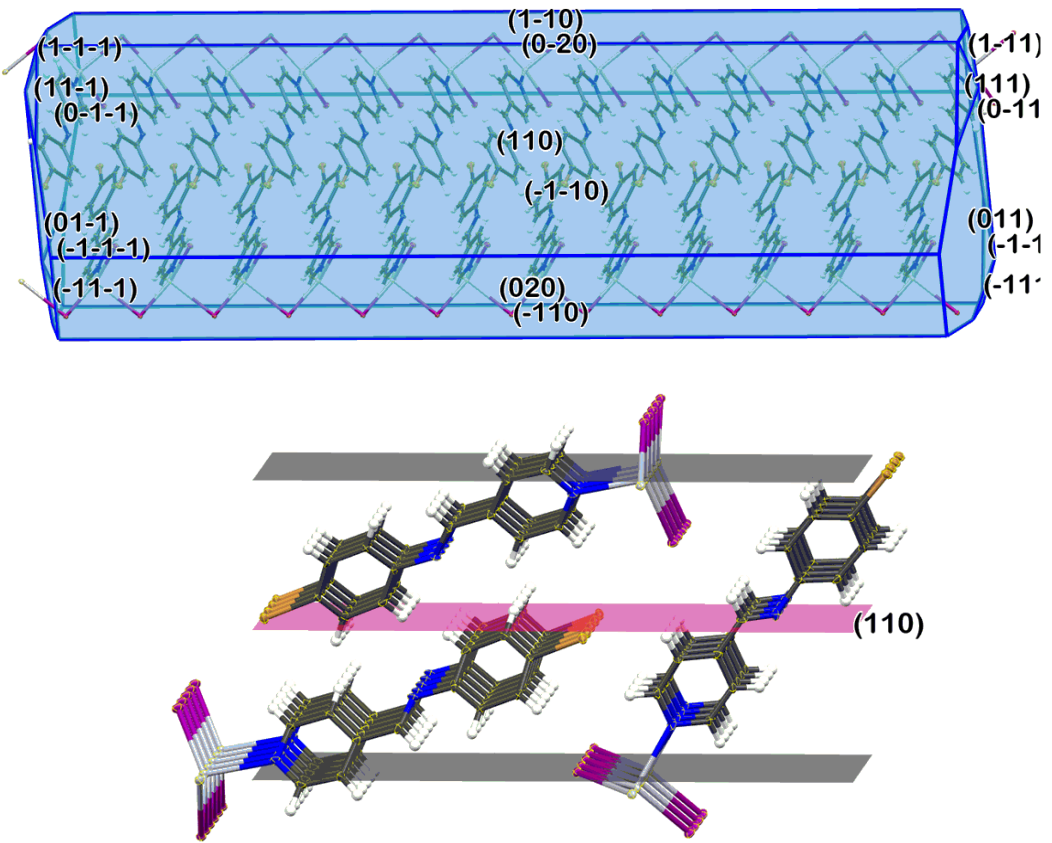
(d)



(e)



(f)



(g)

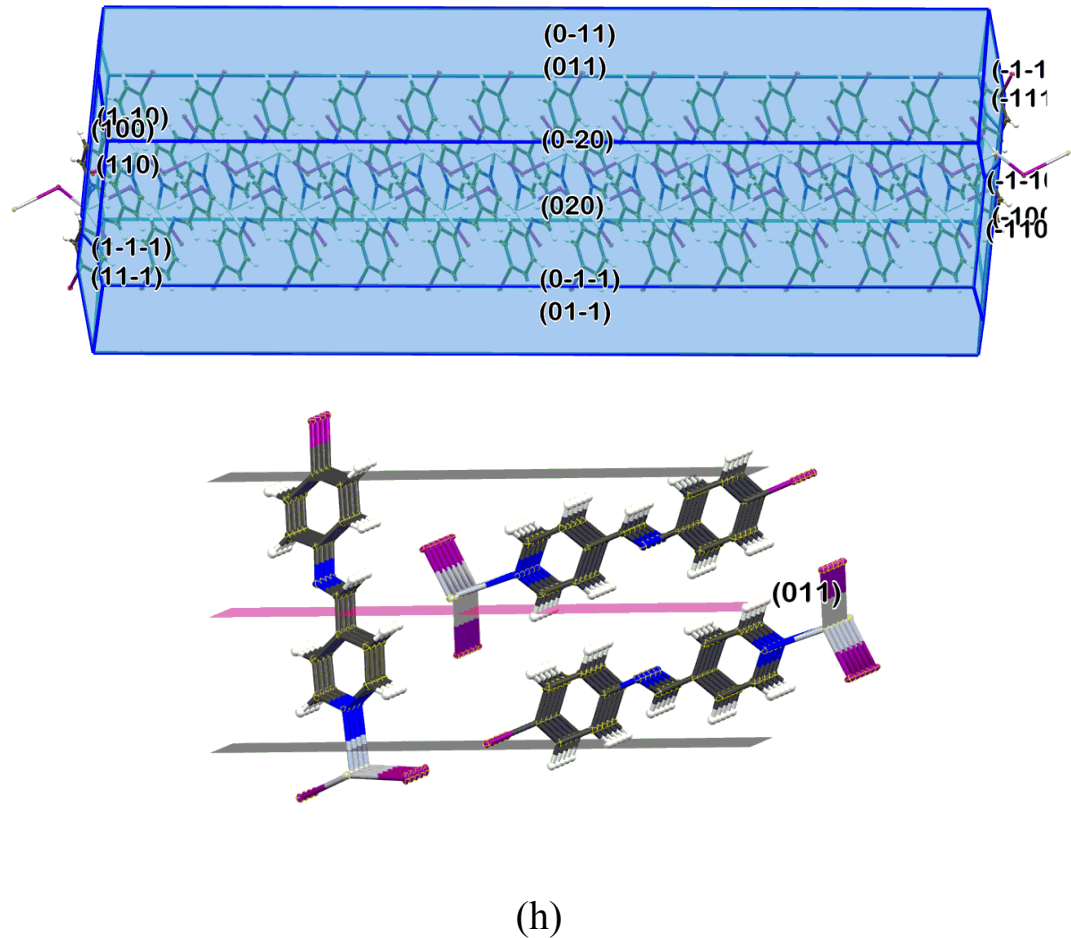
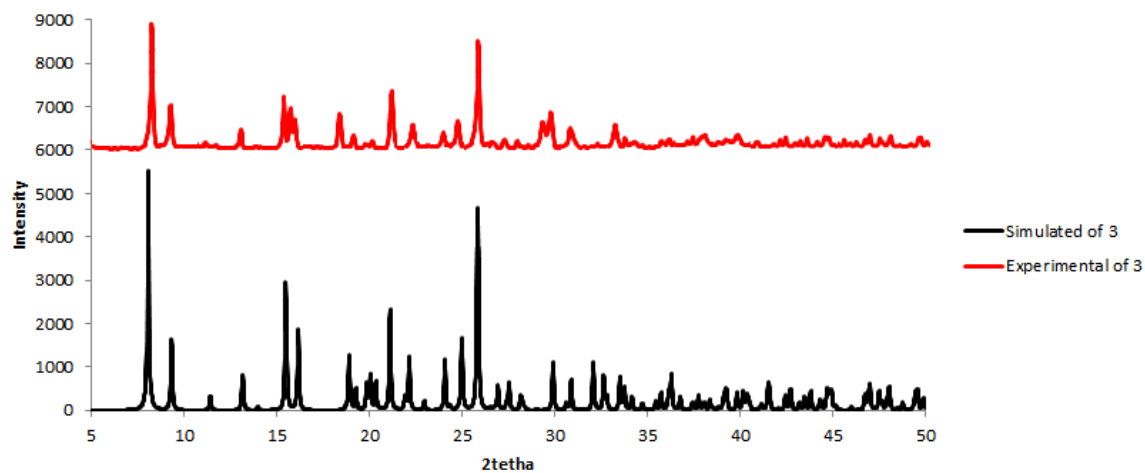
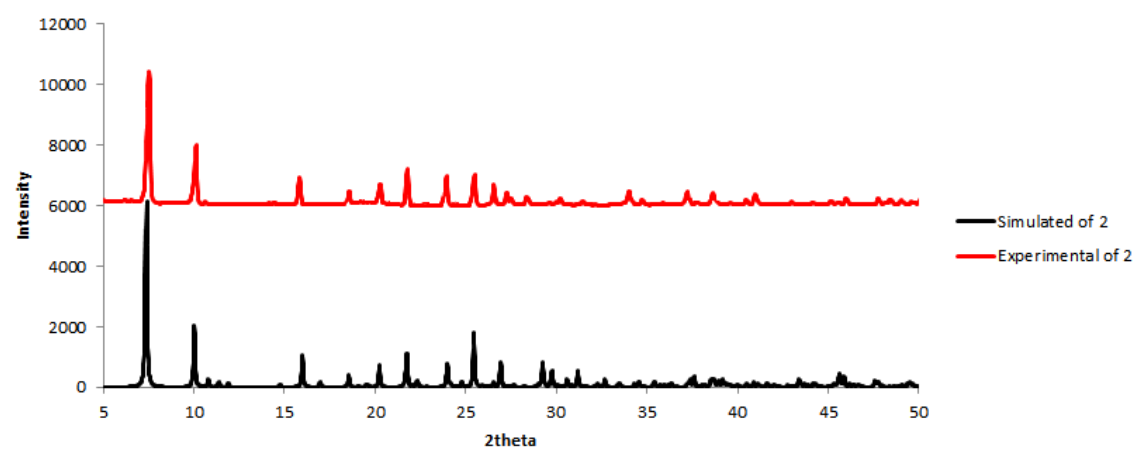
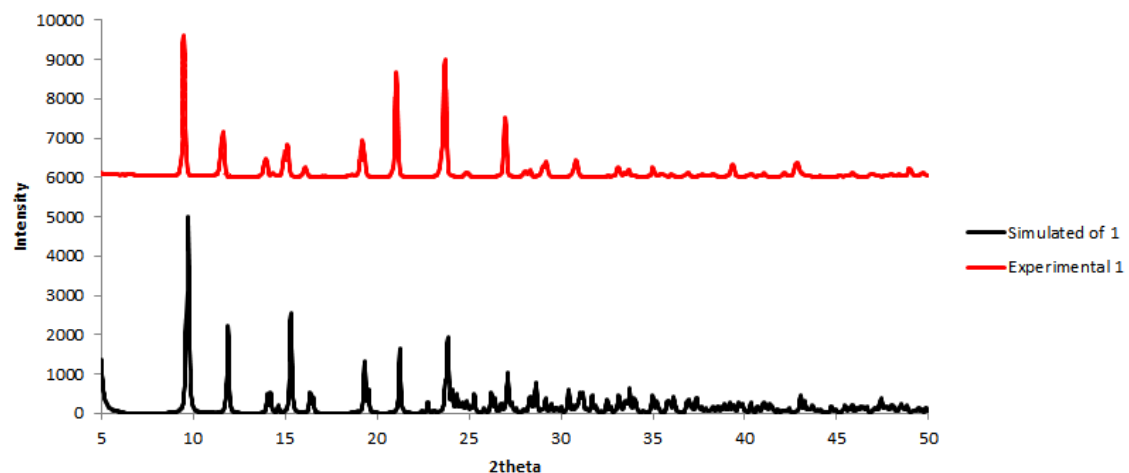
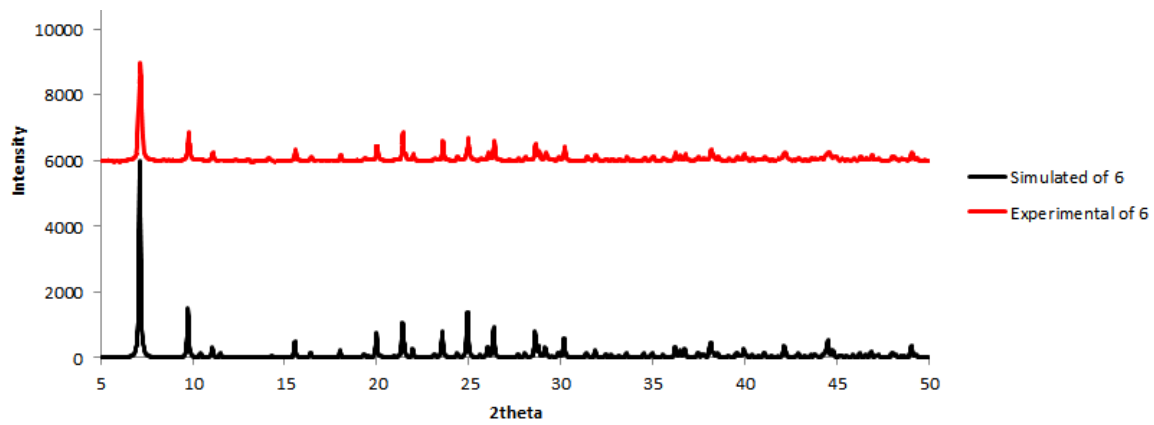
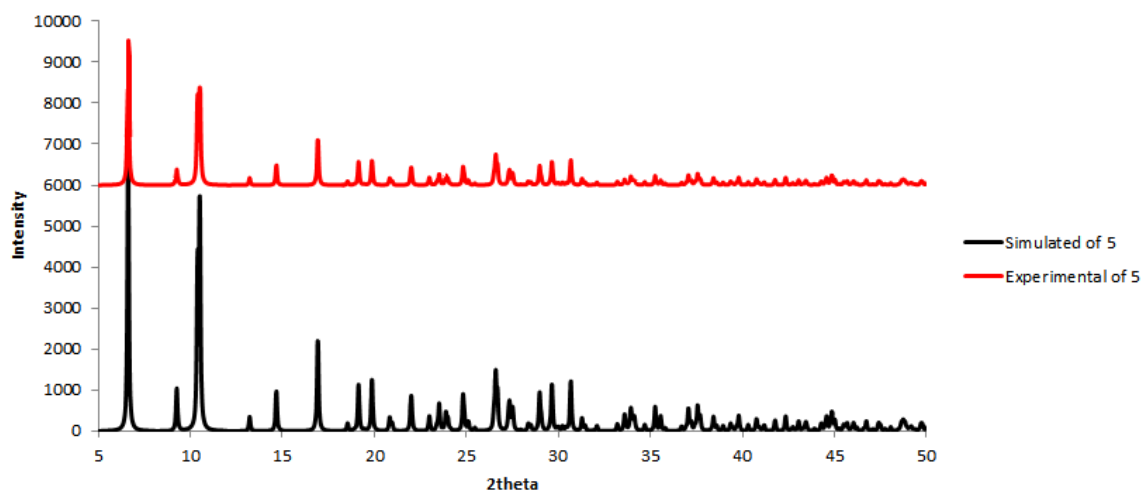
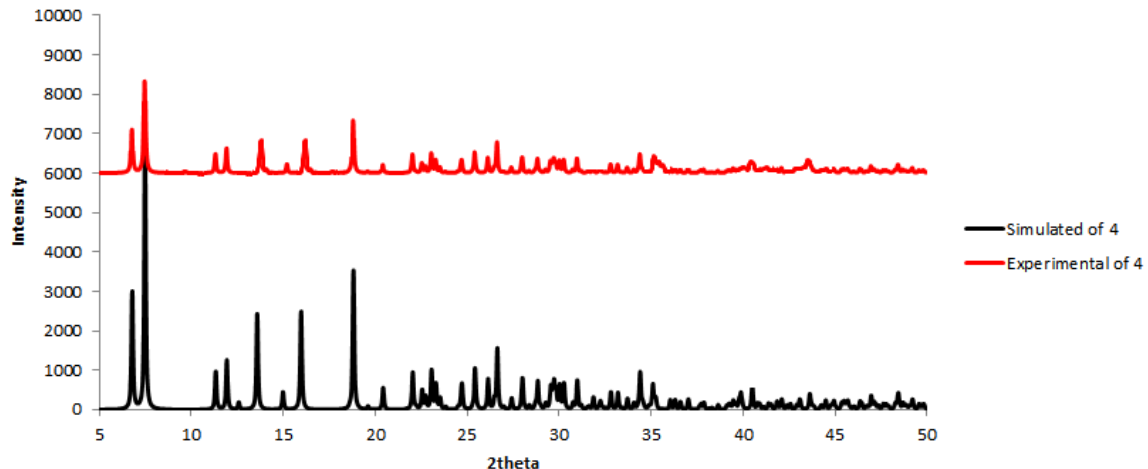


Figure S6. Predicted crystal morphologies of complexes **1-8** and their packing along the [001] for **1** (a), [011] for **2** (b), [220] for **3** (c), [011] for **4** (d), [220] for **5** (e), [011] for **6** (f), [110] for **7** (g) and [011] for **8**, respectively.





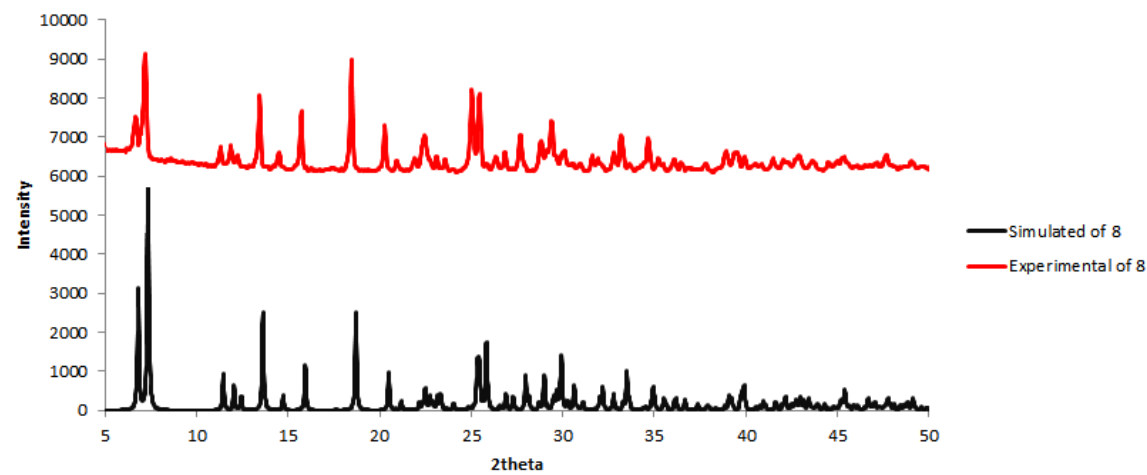
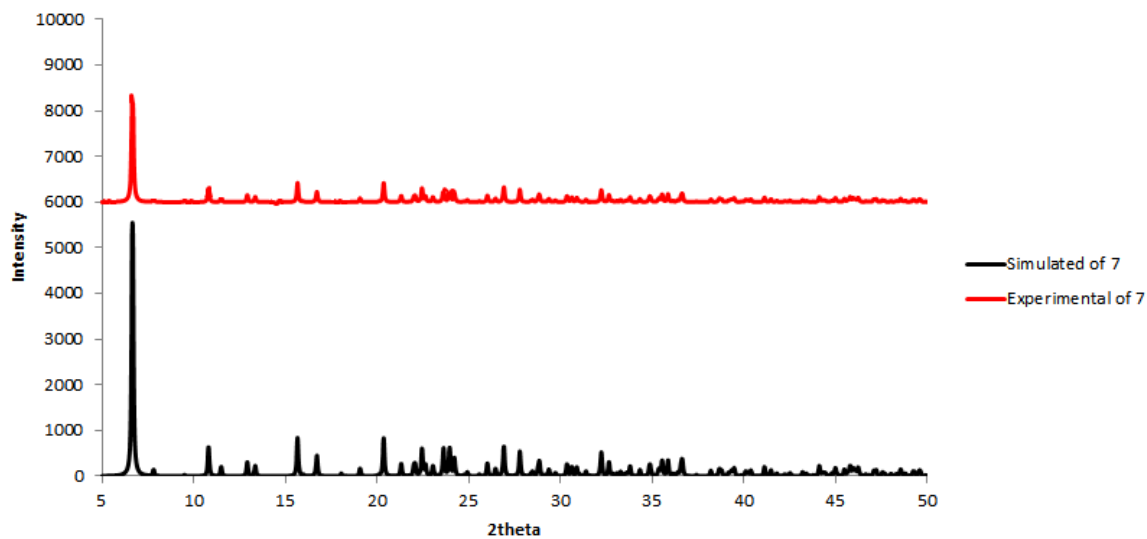


Figure S7. A comparison between simulated XRD pattern of single-crystal X-ray data (black) and the XRD pattern of nanostructures **1-8** (red).

Table S1. Hydrogen bond geometries for complexes **1-8**.

Compound	D-H...A	d(D-H)/Å	d(H...A)/Å	d(D...A)/Å	\angle D-H...A/°	Sym. Code
1	C13A-H13A...F12A	0.950	2.56(2)	3.42(3)	151.2(8)	$2-x,-y,-z$
	C11B-H11B...F12B	0.950	2.52(3)	3.32(3)	142.2(2)	$4-x,1-y,-z$
	C3A-H3A...Br2B	0.950	2.95(2)	3.85(2)	157.5(9)	$x,-1+y,z$
	C5B-H5B...Br1A	0.950	3.03(5)	3.70(2)	128.4(6)	$2-x,1-y,-1-z$
	C11A-H11A...N8B	0.950	2.59 (2)	3.49(3)	158.2(5)	$2-x,1-y,-z$
	C6B-H6B...Br1B	0.950	3.03(6)	3.73(2)	131.15(8)	$x,y,,z$
	C2A-H6A...Br1A	0.950	2.95(4)	3.63(2)	129.22(8)	$x,y,,z$
2	C6-H6...Cl12	0.950	2.828(2)	3.559(7)	150.9(4)	$2-x,\frac{1}{2}+y,1.5-z$
	C10-H10...Br1	0.950	3.039(2)	3.672(8)	125.3(4)	$1.5-x,2-y,1/2+z$
	C2-H2...Br1	0.950	3.135(1)	3.513(7)	105.7(3)	$1+x,y,z$
	C6-H6...Br2	0.950	2.99(4)	3.651(8)	127.5(4)	$x,y,,z$
3	C11-H11...Br1	0.950	2.90(7)	3.71(1)	143.2(2)	$\frac{1}{4}+x,1.75-y,1.75+z$
	C6-H6...Br1	0.950	3.177(2)	3.47(1)	99.8(9)	$-x,2-y,1+z$
	C2-H2...Br1	0.950	3.05(6)	3.72(1)	127.93(5)	$x,y,,z$
4	C3-H3...Br2	0.950	3.109(2)	3.84(3)	135.0(8)	$1+x,1/2-y,1/2+z$
	C11-H11...Br2	0.950	3.051(2)	3.95(3)	157.0(1)	$-x,1-y,2-z$
	C13-H13...I12	0.950	3.188(2)	4.01(3)	146.0(5)	$1-x,1-y,3-z$
	C6-H6...Br2	0.950	3.065(3)	3.73(3)	129.0(8)	$x,y,,z$
5	C5-H5...I1	0.950	3.0755(3)	4.01(1)	166.8(3)	$\frac{1}{4}+x,1.75-y,3/4+z$
	C6-H6...F12	0.950	2.554(3)	3.14(1)	120.4(4)	$\frac{1}{4}-x,-\frac{1}{4}+y,3/4+z$
	C6-H6...I2	0.950	3.2265(8)	3.93(1)	132.4(7)	$x,y,,z$
6	C2-H2...I1	0.950	3.272(2)	3.66(2)	166.9(8)	$-1+x,y,z$
	C5-H5...I1	0.950	3.171(2)	4.01(2)	148.2(9)	$1.5-x,2-y,-\frac{1}{2}+z$
	C10-H10...I1	0.950	3.271(2)	3.92(2)	127.0(1)	$1/2-x,2-y,-\frac{1}{2}+z$
	C11-H11...I2	0.950	3.25(2)	3.80(2)	118.5(1)	$1-x,1/2+y,1/2-z$
	C6-H6...Cl12	0.950	3.027(5)	3.78(2)	137.3(5)	$1-x,1-y,-z$
	C6-H6...I2	0.950	3.148(10)	3.834(15)	130.4(10)	$x,y,,z$
7	C6-H6...Br12	0.950	3.034(4)	3.75(1)	133.7(1)	$1-x,-1-y,1/2+z$

	C11-H11...I2	0.950	3.279(7)	4.19(1)	161.3(1)	$1.5-x,-1/2+y,$ $1/2+z$
	C2-H2...I2	0.950	3.1502(7)	3.82(1)	129.1(7)	x, y, z
	C6-H6...I1	0.950	3.894(11)	3.89(1)	131.8(7)	x, y, z
8	C13-H13...I12	0.950	3.141(9)	3.98(2)	147.5(9)	$2-x, -y, 1-z$
	C14-H14...I1	0.950	3.356(3)	3.74(2)	107.0(4)	$1+x, 1/2-y,$ $-1/2+z$
	C6-H6...I2	0.950	3.17(2)	3.87(2)	132.3(8)	x, y, z

Table S2. Relative contributions of various non-covalent contacts to the Hirshfeld surface area in complexes **1-8**.

Compound	H···H	C···H	C···C	H···N	X···H	X···C	X···X
1	19.8	15.8	5.9	6.7	Br···H=19.9 F···H=10.6	Br···C=0.9 F···C=1.0	Br···Br=3.9 F···F=1.3
2	22.6	7.6	5.6	1.9	Cl···H=11.4 Br···H=24.2	Br···C=2.1 Cl···C=4.4	1.3
3	28.5	9.0	5.9	2.4	28.8	6.1	2.7
4	17.0	16.1	5.2	5.6	Br···H=22.0 I···H=9.6	Br···C=1.5 I···C=0.9	I···Br=7.2 I···I=1.6
5	15.0	17.2	4.2	6.4	F···H=11.1 I···H=24.7	I···C=1.5 F···C=0.4	I···I=4.0 I···F=2.0
6	22.1	6.8	5.1	1.7	I···H=25.8 Cl···H=10.5	Cl···C=4.5 I···C=2.0	I···I=2.0 I···Cl=2.6
7	13.6	17.5	3.9	7.7	Br···H=15.2 I···H=21.8	I···C=1.9 Br···C=1.0	I···Br=0.4 I···I=4.1
8	16.0	17.1	3.9	5.8	30.6	3.1	11.2

Table **S3**. Face lists generated according to the BFDH law using materials studio package.²

Complex 1					
hkl	multiplicity	dhkl	distance	Total facet area	% total facet area
{ 0 0 1}	2	18.40978596	5.43189368	859.80346835	37.84180533
{ 0 1 0}	2	18.16295529	5.50571195	834.94471560	36.74771800
{ 0 1 -1}	2	14.92009488	6.70237025	343.85972328	15.13400816
{ 0 1 1}	2	11.56901523	8.64377806		
{ 0 1 -2}	2	9.18469192	10.88768146		
{ 0 2 -1}	2	9.09226954	10.99835411		
{ 0 1 2}	2	7.49262609	13.34645541		
{ 0 2 1}	2	7.44219739	13.43689166		
{ 0 1 -3}	2	6.30977763	15.84841905		
{ 0 3 -1}	2	6.23017835	16.05090488		
{ 0 2 -3}	2	5.79847756	17.24590619		

Complex 2					
hkl	multiplicity	dhkl	distance	Total facet area	% total facet area
{ 0 1 1}	4	12.02612319	8.31523164	2.527740e+003	78.18682493
{ 0 0 2}	2	8.83865000	11.31394500	133.02762626	4.11474552
{ 0 2 0}	2	8.20425000	12.18880458		
{ 0 1 2}	4	7.78152176	12.85095681		
{ 0 2 1}	4	7.44182154	13.43757028		
{ 0 1 3}	4	5.54569009	18.03202097		
{ 0 3 1}	4	5.22510691	19.13836439		
{ 0 2 3}	4	4.78595466	20.89447291		
{ 0 3 2}	4	4.65100681	21.50072104		
{ 1 0 1}	4	4.55302384	21.96342553	324.94155965	10.05093350
{ 1 1 0}	4	4.52895735	22.08013728	247.23965123	7.64749605

Complex 3					
hkl	multiplicity	dhkl	distance	Total facet area	% total facet area
{ 2 2 0}	4	10.96988247	9.11586794	2.051103e+003	62.36649705
{ 0 4 0}	2	9.47945000	10.54913523	595.37163713	18.10306466
{ 2 4 0}	4	7.74839451	12.90589939		
{ 4 0 0}	2	6.72502500	14.86983320		
{ 4 2 0}	4	6.33809524	15.77761081		
{ 2 6 0}	4	5.71972735	17.48335085		
{ 1 1 1}	4	4.69188659	21.31338812	321.15747343	9.76521914
{ 1 1 -1}	4	4.69188659	21.31338812	321.15747343	9.76521914
{ 4 6 0}	4	4.60530561	21.71408555		
{ 2 8 0}	4	4.47028117	22.36995757		
{ 1 3 1}	4	4.42849715	22.58102390		

Complex 4					
hkl	multiplicity	dhkl	distance	Total facet area	% total facet area
{ 0 1 1}	4	13.04252649	7.66722614	1.931979e+003	63.21719835
{ 0 2 0}	2	11.82850000	8.45415733	684.50235792	22.39792073
{ 0 2 1}	4	9.43266369	10.60145928		
{ 0 0 2}	2	7.81649299	12.79346123		
{ 0 1 2}	4	7.42186114	13.47370938		
{ 0 3 1}	4	7.04064911	14.20323586		
{ 0 3 2}	4	5.55139018	18.01350595		
{ 0 4 1}	4	5.53162612	18.07786678		
{ 0 1 3}	4	5.08899818	19.65023301		
{ 0 2 3}	4	4.76874249	20.96988888		
{ 0 5 1}	4	4.52853682	22.08218770		

Complex 5					
hkl	multiplicity	dhkl	distance	Total facet area	% total facet area
{ 2 2 0}	4	13.42118163	7.45090878	2.653416e+003	84.52958599
{ 0 4 0}	2	9.58145000	10.43683367	35.92364348	1.14441555
{ 4 0 0}	2	9.40152500	10.63657226		
{ 2 4 0}	4	8.53698432	11.71373828		
{ 4 2 0}	4	8.44044031	11.84772314		
{ 2 6 0}	4	6.04816667	16.53393589		
{ 6 2 0}	4	5.95713838	16.78658335		
{ 4 6 0}	4	5.28351495	18.92679418		
{ 6 4 0}	4	5.24513597	19.06528267		
{ 2 8 0}	4	4.64241269	21.54052357		
{ 8 2 0}	4	4.56540789	21.90384788		

Complex 6					
hkl	multiplicity	dhkl	distance	Total facet area	% total facet area
{ 0 1 1}	4	12.40143207	8.06358487	2.448384e+003	78.94120030
{ 0 0 2}	2	9.07775000	11.01594558	115.52453958	3.72476080
{ 0 2 0}	2	8.49000000	11.77856302		
{ 0 1 2}	4	8.00551754	12.49138478		
{ 0 2 1}	4	7.69066255	13.00278089		
{ 0 1 3}	4	5.70058804	17.54204991		
{ 0 3 1}	4	5.40350725	18.50649871		
{ 0 2 3}	4	4.92799564	20.29222573		
{ 0 3 2}	4	4.80290008	20.82075376		
{ 1 0 1}	4	4.60347647	21.72271339	301.88554940	9.73344247
{ 1 1 0}	4	4.58242330	21.82251474	235.73470897	7.60059643

Complex 7					
hkl	multiplicity	dhkl	distance	Total facet area	% total facet area
{ 1 1 0}	4	13.25262428	7.54567532	2.041987e+003	67.72742026
{ 0 2 0}	2	11.30715000	8.84396156	531.06165012	17.61393564
{ 1 2 0}	4	9.30085856	10.75169560		
{ 2 0 0}	2	8.17770000	12.22837717		
{ 2 1 0}	4	7.69032570	13.00335043		
{ 1 3 0}	4	6.84596728	14.60713964		
{ 2 3 0}	4	5.54258301	18.04212944		
{ 1 4 0}	4	5.34334792	18.71485845		
{ 3 1 0}	4	5.29996236	18.86805853		
{ 3 2 0}	4	4.91078718	20.36333408		
{ 1 5 0}	4	4.35924946	22.93972870		

Complex 8					
hkl	multiplicity	dhkl	distance	Total facet area	% total facet area
{ 0 1 1}	4	12.99369606	7.69603964	1.807601e+003	61.47028127
{ 0 2 0}	2	12.03060000	8.31213738	694.97455799	23.63369626
{ 0 2 1}	4	9.48953920	10.53791949		
{ 0 0 2}	2	7.71920099	12.95470867		
{ 0 1 2}	4	7.35021190	13.60504994		
{ 0 3 1}	4	7.11726138	14.05034811		
{ 0 4 1}	4	5.60487901	17.84159832		
{ 0 3 2}	4	5.56173320	17.98000666		
{ 0 1 3}	4	5.03232339	19.87153692		

References

- 1) Wong, W-Y.; Wong, W-T. *J. Organomet. Chem.*, 1999, 584, 48–57
- 2) Yao, W.; Yan, Y. L.; Xue, L.; Zhang, C.; Li, G. P.; Zheng, Q. D.; Zhao, Y. S.; Jiang, H.; Yao, J. N. *Angew. Chem., Int. Ed.*, 2013, 52, 8713.